Journal of Hazardous Materials 162 (2009) 1086–1098

Contents lists available at ScienceDirect

Journal of Hazardous Materials

journal homepage: www.elsevier.com/locate/jhazmat

Fixed-bed column study for hexavalent chromium removal and recovery by short-chain polyaniline synthesized on jute fiber

Potsangbam Albino Kumar, Saswati Chakraborty*

Department of Civil Engineering, Indian Institute of Technology Guwahati, Assam 781039, India

ARTICLE INFO

Article history:
Received 31 January 2008
Received in revised form 29 May 2008
Accepted 30 May 2008
Available online 5 June 2008

Keywords:
Chromium
Polyaniline
Breakthrough curve
BDST model
Dynamic bed capacity

ABSTRACT

Fixed-bed column studies were conducted to evaluate performance of a short-chain polymer, polyaniline, synthesized on the surface of jute fiber (PANI-jute) for the removal of hexavalent chromium [Cr(VI)] in aqueous environment. Influent pH, column bed depth, influent Cr(VI) concentrations and influent flow rate were variable parameters for the present study. Optimum pH for total chromium removal was observed as 3 by electrostatic attraction of acid chromate ion ($HCrO_4^-$) with protonated amine group (NH_3^+) of PANI-jute. With increase in column bed depth from 40 to 60 cm, total chromium uptake by PANI-jute increased from 4.14 to 4.66 mg/g with subsequent increase in throughput volume from 9.84 to 12.6 L at exhaustion point. The data obtained for total chromium removal were well described by BDST equation till 10% breakthrough. Adsorption rate constant and dynamic bed capacity at 10% breakthrough were observed as 0.01 L/mg h and 1069.46 mg/L, respectively. Adsorbed total chromium was recovered back from PANI-jute as non-toxic Cr(III) after ignition with more than 97% reduction in weight, minimizing the problem of solid waste disposal.

1. Introduction

Rapid industrialization over the years led to an increase and accumulation of hexavalent chromium in environment. Chromium exists in environment as trivalent [Cr(III)] and hexavalent [Cr(VI)] forms and Cr(VI) is considered highly toxic, carcinogenic and mutanogenic. WHO (World Health Organization) and BIS (Bureau of Indian Standards) recommended guideline value for chromium (as total chromium) in drinking water as 0.05 mg/L (desirable) with no relaxation on permissible limit [1,2]. Anthropogenic source of chromium is generally from various industrial processes like electroplating, leather tanning, wood preservations, manufacturing of dye, paint and paper [3]. Several physicochemical wastewater treatment processes have been developed and reported to remove hexavalent chromium. These include chemical reduction followed by precipitation [4,5], electrochemical precipitation [6], ion exchange [7], solvent extraction [8], evaporation, reverse osmosis, foam separation, adsorption, biosorption [9,10], etc. Most of these methods like solvent extraction, reverse osmosis, ion exchange, electrochemical precipitation, etc., need high capital cost and recurring expenses such as chemicals, which are not suitable for small-scale industries. Reduction of Cr(VI) to Cr(III) and then employing chemical precipitation, though economical, generates large amount of toxic sludge making disposal difficult. The process of adsorption is by far the most versatile and widely used technique for the removal of hexavalent chromium. Several researchers investigated adsorption of chromium using certain easily available low cost materials such as rice bran, wool, sawdust, etc. [11–13]. However, low adsorption capacity and slow kinetics of these adsorbents created a necessity to develop innovative low cost adsorbents having strong affinity towards metal ions and ability to remove heavy metals in a relatively short period of time.

Since the last decade, adsorption of metal ions by several functionalized polymers based on amines derivatives such as polyacrylonitrile fibers, ethylenediamine, polyacrylamides, poly-4-vinylpyridine, polyethyleneimine, aniline formaldehyde condensate, etc., have been reported [14–19]. Recently, we have investigated one amine-based polymer, short-chain polyaniline coated on jute fiber for the removal of chromium in batch mode [20]. Maximum adsorption of total chromium [Cr(VI) and Cr(III)] was observed at reaction pH of 3 and adsorption equilibrium was achieved within 40–120 min for initial Cr(VI) of 50–500 mg/L. Batch data has several limitations to predict the performances in practical situation such as actual industrial wastewater treatment plant, where continuous reactors replace batch operation. It was also observed that literatures on chromium ion removal by polymers in fixed-bed mode are very scanty.

* Corresponding author. Tel.: +91 361 2582412; fax: +91 361 2690762.
E-mail addresses: saswati@iitg.ernet.in, chakraborty_saswati@hotmail.com (S. Chakraborty).

0304-3894/$ – see front matter © 2008 Elsevier B.V. All rights reserved.
doi:10.1016/j.jhazmat.2008.05.147

Nomenclature

A	cross-sectional area (m^2)
b	energy (heat) constant of adsorption (L/mg)
C	concentration of adsorbate at any instance of time t (mg/L)
C_b	concentration of adsorbate in effluent at breakthrough concentration (mg/L)
C_E	concentration of adsorbate in effluent at exhaustion (mg/L)
C_e	equilibrium concentration (mg/L)
C_0	initial concentration of adsorbate (mg/L)
dh	differential depth of column (cm)
h	hour
h_z	height of adsorption zone (cm)
I	influent adsorbate loading (mg)
k_{ads}	adsorption rate constant (L/mg h)
k_{TH}	Thomas model rate constant (mL/min mg)
K_o	overall mass transfer coefficient ($ML^{-2}T^{-1}$)
min	minute
M	mass of adsorbate not removed (mg)
M_r	mass of adsorbate removed (mg)
M_d	mass of adsorbate desorbed (mg)
N_o	dynamic bed capacity (mg/L)
q_e	amount of adsorbate uptake (mg/g)
q_m	Langmuir's maximum monolayer coverage (mg/g)
Q	volumetric flow rate (mL/min)
Q_o	maximum solid phase concentration of solute (mg/g)
t	flow time (min)
t_B	breakthrough time (h)
t_E	exhaust time (h)
t_S	service time (h)
u	linear flow rate (cm/h)
V_B	throughput volume at breakthrough (L)
V_E	throughput volume at exhaust (L)
V_t	throughput volume at any instant of time t (L)
Z	column depth (cm)
Z_o	critical bed depth (cm)

Greek letter

α	external surface area

In the present work, short-chain polymer named polyaniline was used for the removal of chromium ion in continuous mode. This polymer was synthesized on the surface of jute fiber to facilitate separation of metal ion after metal–polymer interaction. Jute fiber was selected due to its easy availability in local market and lower cost. Influent pH, column bed depth, influent Cr(VI) concentrations, influent flow rates and recovery of chromium were selected as variable factors for the present work.

2. Theoretical background

2.1. Column performance

The performance of the column bed is usually described through the concept of breakthrough curve, which is obtained by plotting throughput volume (V_t) at any time (t) versus effluent chromium concentration (C). Throughput volume was calculated using Eq. (1).

$$V_t = Qt \tag{1}$$

where Q is the volumetric flow rate (mL/min). Usually breakthrough is defined as phenomenon when concentration from column is about 3% to 5% [21,22]. However, breakthrough at 1% was also considered and reported on basis of effluent discharge limit for specific metal [23]. Employment of breakthrough of 50% was also reported for the removal of lead(II) using treated granular activated carbon [24]. For our study, the breakthrough time was obtained for total chromium concentration of 0.1 mg/L (1%) considering the permissible limit for total chromium discharge.

Exhaustion is usually considered when the effluent concentration remains same for long period close to influent concentration. Vijayagarvan et al. [23] considered exhaustion at 99% and above of influent for the removal of copper by brown marine alga *Turbinaria ornata*. Adak and Pal [25] considered exhaustion when effluent reached 90% of influent on removing phenols by SDS-modified alumina. For our studies, exhaustion was considered when effluent chromium reached 95% of influent concentration [26]. Area below the breakthrough curve represents mass of chromium which is not removed (M) and was calculated using Eq. (2) [27]:

$$M = \sum \left[\frac{(V_{n+1} - V_n)(C_{n+1} + C_n)}{2} \right] \tag{2}$$

where V_n is the throughput volume at nth reading (L), V_{n+1} the throughput volume at $(n+1)$th reading (L), C_n the effluent adsorbate concentration at nth reading (mg/L) and C_{n+1} is the effluent adsorbate concentration at $(n+1)$th reading (mg/L).

Influent adsorbate load (I) was calculated from throughput volume (V_E) at column exhaustion and influent adsorbate concentration (C_o) according to Eq. (3).

$$\text{influent adsorbate load (mg)} = I = V_E C_o \tag{3}$$

Mass of adsorbate removed was calculated from difference of influent adsorbate load (I) and mass of adsorbate not removed (M) from Eq. (4).

$$\text{mass of adsorbate removed} = M_r\,(\text{mg}) = I - M \tag{4}$$

Adsorbate uptake by PANI-jute was calculated using Eq. (5).

$$\text{adsorbate uptake by PANI-jute}\,(q_e) = \frac{M_r\,(\text{mg})}{\text{PANI-jute weight (g)}} \tag{5}$$

2.2. Bed depth service time (BDST) model

Over the years, several mathematical models have been developed for analyzing the lab-scale column studies to design pilot scale columns [22,28,29]. One of the most applied models for adsorption of heavy metals on column studies is the bed depth service time (BDST) model based on Bohart–Adams equation [30]. The Bohart–Adams equation can be represented as:

$$\ln\left(\frac{C_o}{C_b} - 1\right) = \ln(e^{k_{ads}N_o(Z/u)} - 1) - k_{ads}C_o t_S \tag{6}$$

Further, Hutchin [31] modified the Bohart–Adams equation and presented a linear relationship between the bed depth and service time [Eq. (7)], which requires only three fixed-bed tests to collect the necessary data.

$$t_S = \frac{N_o Z}{C_o u} - \frac{1}{k_{ads}C_o}\ln\left(\frac{C_o}{C_b} - 1\right) \tag{7}$$

where t_S is the service time at breakthrough point (h), N_o the dynamic bed capacity (mg L^{-1}), Z the packed-bed column depth (cm), u the linear flow rate (cm/h) defined as the ratio of the volumetric flow rate Q (cm^3/h) to the cross-sectional area of the bed A (cm^2), C_o and C_b are, respectively, the influent and the breakthrough adsorbate concentration (mg/L) and k_{ads} is the adsorption rate constant (L/mg h). Plotting service time (t_S) versus bed depth

(Z) will generate a straight line equation having slope of ($N_o/C_o u$) and intercept of

$$(-)\frac{1}{k_{ads}C_o}\ln\left(\frac{C_o}{C_b}-1\right).$$

Critical bed depth (Z_o) represents the theoretical minimum depth of adsorbent that would be able to prevent the adsorbate concentration from exceeding C_b. It is obtained when breakthrough is immediate and it can be calculated by substituting $t_S = 0$ in Eq. (7) as shown below:

$$Z_o = \frac{u}{k_{ads}N}\left(\frac{C_o}{C_b}-1\right) \tag{8}$$

According to BDST model Eq. (7), the data collected from one flow rate experiment can predict the system with different flow rate. When an experiment conducted at flow rate Q_1, yields an equation of the form

$$t_S = a_1 Z + b_1 \tag{9a}$$

the predicted equation for new flow rate Q_2, is given by:

$$t_S = a_2 Z + b_1 \tag{9b}$$

and

$$a_2 = a_1\left(\frac{Q_1}{Q_2}\right) \tag{9c}$$

where a_1 and a_2 are the slopes at flow rate Q_1 and Q_2, respectively. However, the intercept b_1 remained same since it is independent of flow rate in linearized BDST Eq. (7).

BDST model can also be used to design systems for treating other influent solute concentrations using the data of a previous laboratory experiment of one influent solute concentration. When an experiment conducted at initial concentration C_1, yields an equation of the form

$$t = r_1 X + s_1 \tag{10a}$$

the predicted equation for new flow rate Q_2, is given by:

$$t = r_2 X + s_2 \quad \text{and} \tag{10b}$$

The new slope and intercept values can be determined as:

$$r_2 = r_1\left(\frac{C_1}{C_2}\right) \tag{10c}$$

$$s_2 = s_1\frac{C_1}{C_2}\left(\frac{\ln\left[(C_2/C_F)-1\right]}{\ln\left[(C_1/C_b)-1\right]}\right) \tag{10d}$$

where r_1 and r_2 are slopes at influent concentrations C_1 and C_2, respectively; s_1 and s_2 are intercepts at influent concentrations C_1 and C_2, respectively; C_F is effluent concentration at influent concentrations C_2; and C_b is effluent concentration at influent concentration C_1.

2.3. Thomas model

Another mathematical model Thomas equation is given by [32]

$$\frac{C_o}{C} = 1+\exp\left(\frac{k_{TH}}{Q}(Q_o M - C_o V_t)\right) \tag{11}$$

where C_o is the initial adsorbate concentration (mg/L), C the effluent adsorbate concentration (mg/L), k_{TH} the Thomas model rate constant (mL min^{-1} mg^{-1}), Q_o the maximum solid-phase concentration of the solute (mg/g) and V_t is the throughput volume. Linearized form of Thomas model is as follows:

$$\ln\left(\frac{C}{C_o}-1\right) = \frac{k_{TH}Q_o M}{Q} - \frac{k_{TH}C_o}{Q}V_t \tag{12}$$

Thomas model assumes Langmuir kinetics of adsorption–desorption and no axial dispersion. It is derived with the adsorption that the rate driving force obeys second-order reversible reaction kinetics.

2.4. Theoretical breakthrough curve

The breakthrough curve of a continuous fixed-bed operation mode can also be obtained using the data obtained from the batch isotherm studies. Thus, column operation can be designed from batch experiment data without running the column experiment and the procedure is given below:

(i) An operating line needs to be drawn passing through the origin and intersecting the equilibrium curve (C_e versus q_e of batch data) at C_o (designed influent adsorbate concentration of column bed experiment to be conducted). The significance of this operating line was that the data of continuously mixed batch reactor and the data of fixed-bed reactor are identical at these two points, first at the initiation and other at the exhaustion of the reaction [33].

(ii) The rate of transfer of the adsorbate from the solution over a differential depth of column dh is given by

$$Q\,\mathrm{d}C = K_o\alpha(C-C_e)\mathrm{d}h \tag{13}$$

where Q is the flow rate, K_o the overall mass transfer coefficient (ML^{-2}T^{-1}), α the external surface area, C_e the equilibrium concentration of the adsorbate in the solution corresponding to a adsorbed concentration q_e and C is the concentration of the adsorbate at a given instant of time t [34].

(iii) The term $(C-C_e)$ is the driving force for adsorption and is equal to the difference between the operating line and equilibrium curve at any given q_e value. Integrating Eq. (13) and solving for the height of adsorption zone (h_z) at saturation yields

$$h_z = \frac{Q}{K_o\alpha}\int_{C_b}^{C_E}\frac{\mathrm{d}c}{(C-C_e)} \tag{14}$$

where C_b and C_E are the concentrations of adsorbate in effluent at breakthrough and at exhaustion point, respectively.

(iv) The area under the curve of C versus $(C-C_e)^{-1}$ represented the value of the above integration. Since, $(C-C_e)^{-1}$ approaches infinity as C approaches C_o, it is necessary to terminate the plot of C at a value somewhat less than C_o or at $C = 0.95C_o$ (exhaustion for adsorption beds). For any value of h less than h_z corresponding to a concentration $C_b < C < C_E$, Eq. (14) can be written as

$$h = \frac{Q}{k_o\alpha}\int_{C_b}^{C}\frac{\mathrm{d}c}{(C-C_e)} \tag{15}$$

dividing Eq. (15) by Eq. (14) results in

$$\frac{h}{h_z} = \frac{\int_{C_b}^{C}\mathrm{d}C/(C-C_e)}{\int_{C_b}^{C_E}\mathrm{d}C/(C-C_e)} = \frac{V_t-V_B}{V_E-V_B} \tag{16}$$

where h/h_z is equal to the ratio $(V_t-V_B)/(V_E-V_B)$, where V_B and V_E are throughput volumes at breakthrough and exhaustion, respectively, and V_t is the throughput volume within V_E for an effluent concentration C within C_E (or throughput volume at any instant of time t within exhaustion point). It should be noted that Eq. (16) is valid only if the transfer term $K_o\alpha$ is constant within the adsorption zone for changing concentrations. For most practical applications, this term is sufficiently

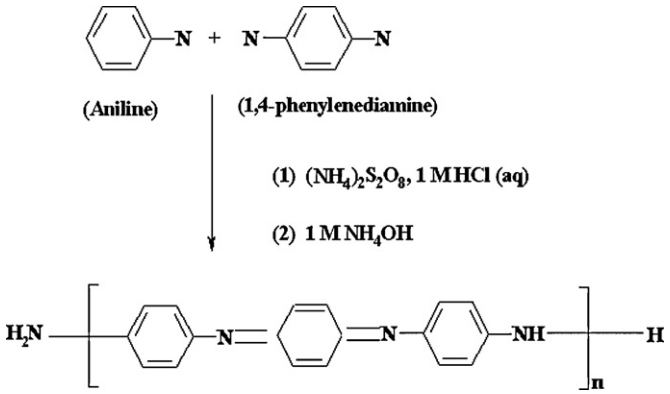

Fig. 1. Synthesis scheme of PANI.

constant to permit use of the relationship for evaluation of the breakthrough curve [34].

(v) Finally, the theoretical breakthrough curves were generated by plotting $(V_t - V_B)/(V_E - V_B)$ versus (C/C_o).

3. Materials and methods

3.1. Chemicals and reagents

Commercial grade aniline ($C_6H_5NH_2$) purified by distilling over KOH pellets at 180 °C was used for preparing PANI. Potassium dichromate ($K_2Cr_2O_7$) purchased from Merck, India, and chromic chloride ($CrCl_3{\cdot}6H_2O$) procured from Central drug house, India, were used as the sources of hexavalent and trivalent chromium, respectively. Jute fibers were prepared by washing waste grocery jute bags to remove the dirt and chopped into fibers of length 0.5–1 cm.

3.2. Synthesis of polyaniline on jute fiber

Polyaniline was synthesized by oxidation of aniline ($C_6H_5NH_2$) by oxidant ammonium peroxydisulfate [$(NH_4)_2S_2O_8$] in presence of chain terminating agent 1,4-phenylenediamine in acidic aqueous medium. The synthesis scheme of PANI is shown in Fig. 1 [20,35]. Aniline (2.00 g, 21.5 mmol) and 1,4-phenylenediamine (0.330 g, 3.05 mmol) were dissolved in 66 mL of 1 M HCl (aq.). The mixture was cooled in iced bath which was maintained at 0–5 °C followed by addition of 5 g jute fibers and stirred for 5 min. The polymerization started by introduction of pre-cooled (5 °C) solution of ammonium peroxydisulfate (1.62 g, 7.10 mmol) in 16 mL of 1 M HCl (aq.). The reaction mixture was kept at 5 °C for 65 min and then kept for overnight at room temperature to complete the reaction. Then the liquid was decanted from PANI-jute fiber. To ensure complete deprotonation of PANI-jute, alkali treatment was given by soaking PANI-jute in 1 M NH_4OH for 5 min. The products were then washed with distilled water to adjust the solution to neutral pH. Finally, the blue black colored PANI-jute fiber was dried at 40 °C in the oven. The photographs of raw jute fibers and PANI-jute are shown in figures (Figs. 1 and 2 in supplementary materials).

3.3. Experimental set up

The fixed-bed column studies were conducted using a laboratory-scale glass column of 1 cm ID and 70 cm length. Column was packed with known quantity of PANI-jute to obtain a particular bed depth. A cotton plug was provided at the bottom to support the PANI-jute bed as well as to prevent the washed out of adsorbent. Another cotton plug was also provided on top of the bed to prevent floating up of PANI-jute fibers. The schematic arrangement of the column set up is shown in Fig. 2. The presence of air pockets within the packed PANI-jute caused channeling of influent chromium contaminated solution and lowered the adsorption efficiency of the bed [36]. To ensure expulsions of the trapped air, PANI-jute packed columns were fully wetted by filling with deionised water for 5 h prior to starting of the experiments. In a typical experiment, influent Cr(VI) feed at a particular flow rate was supplied and maintained throughout the experiments by use of peristaltic pump (Model: PA-SF Control , IKA-WERKE, Germany). Flow rate was cross-checked at the exit of the column at regular intervals of 2 h to prevent and minimize the flow rate fluctuations if occurred inside the column bed.

3.4. Column experiment

In order to study the behavior of hexavalent chromium removal in fixed-bed column mode, column experiments were conducted with varying pH, influent concentration, flow rate, and bed depth. Treated solution samples were collected from the exit of column at predetermined time intervals. These samples were then centrifuged at 10,000 rpm for 10 min and analyzed for total chromium [Cr(VI) + Cr(III)] as well as Cr(VI). pH of the effluent samples were also monitored and recorded along. In order to prevent any leakage of toxic chromium into the sewer line, a polishing column of ID 3 cm × 5 cm length packed with PANI-jute was introduced after exit point of column as further polishing unit (Fig. 2).

3.5. Analytical techniques

Total chromium was estimated by atomic absorption spectrophotometer (Spectra AA, Varian Model) using air-acetylene flame at 429 nm wavelength and slit width of 0.5 nm. Sensitivities of atomic absorption spectrophotometer varies with wavelength and slit width. At 429 nm wavelength, the detection limit of total chromium is 1–100 mg/L. Cr(VI) was estimated based on colorimetric method using UV Spectrophotometer (Varian Model, Cary 50) at 540 nm wavelength by 1,5-diphenyl carbazide method. This method can determine Cr(VI) in the range from 0.10 to 1.0 mg/L [37]. Cr(III) was calculated as difference of total chromium and Cr(VI) for

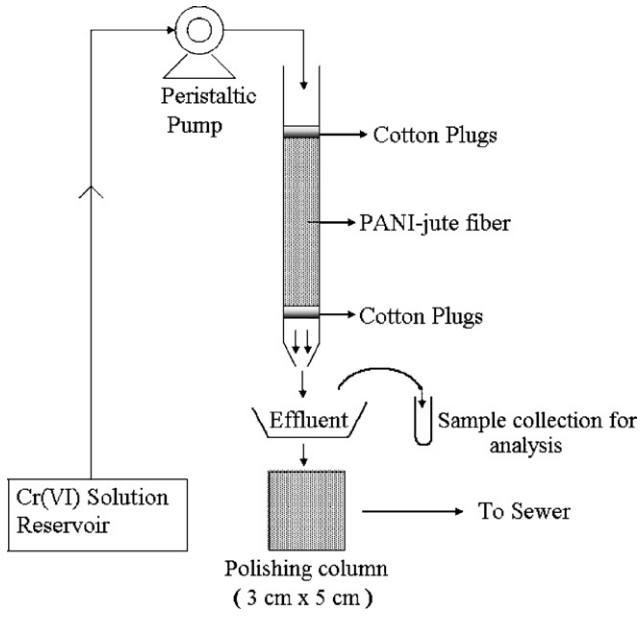

Fig. 2. Schematic arrangement of the experimental set up for fixed-bed studies.

the same sample solution. Change in surface morphology of PANI-jute before and after adsorption of chromium and confirmation of presence of chromate ions on surface of PANI-jute was investigated using scanning electron microscopy (Scanning electron microscope, Model: LEO, 1430 VP, Carl Zeiss, Germany). Presence of adsorbed Cr(III) on PANI-jute was examined by employing electromagnetic spin resonance spectrophotometer (ESR) (Model: JES-FA 200 ESR System, JEOL, Ltd. Japan).

4. Results and discussions

4.1. Effect of influent pH

Effects of influent pH on Cr(VI) removal by PANI-jute was studied by running five columns of 30 cm bed depth (7.05 g PANI-jute) at influent pH 2, 3, 4, 5, and 6. Empty bed residence time (EBRT) was calculated using Eq. (17).

$$\text{EBRT}\,(\text{min}) = \frac{\text{empty bed column volume}\,(\text{m}^3)}{\text{volumetric flow rate}\,(\text{m}^3/\text{min})} \quad (17)$$

Empty bed column volume was calculated from column ID (1 cm) and height of column bed (30 cm) and EBRT was 11.78 min. From our previous studies on removal of Cr(VI) by PANI-jute in batch process, it was observed that Cr(VI) was highly reduced to Cr(III) at acidic pH [20]. Perusals of literature had also reported the reduction of Cr(VI) to Cr(III) at acidic pH along with protons been consumed supported by Eq. (18) [19,20,38,39].

$$HCrO_4^- + 7H^+ + 3e^- \rightarrow Cr^{3+} + 4H_2O \quad E_o = 1.33\,V \quad (18)$$

Hence, throughout the study in column effluent, both Cr(VI) and total chromium were analyzed and Cr(III) was estimated. Also amount of total chromium and Cr(VI) removed till exhaust were calculated separately. Breakthrough curve of Cr(VI) is presented as throughput volume versus effluent Cr(VI) concentration in Fig. 3(a). The column bed exhaustion time (t_E), throughput volume at exhaustion (V_E) of Cr(VI) were evaluated with respect to Cr(VI) exhaustion point [effluent Cr(VI) 19 mg/L] and presented in Table 1. Amount of Cr(VI) removed (M_r) was evaluated from the area above the curve of throughput volume versus effluent Cr(VI) using Eqs. (2)–(4) and shown in Table 1. It can be seen that with the increase in pH, mass of Cr(VI) removed decreased. With decreased in pH from pH 6 to pH 3, respective exhaust time and throughput volume increased from 23 h and 2.76 L to 46 h and 5.52 L with corresponding Cr(VI) removal increased from 4.17 to 33.2 mg. At pH 2, column bed was not exhausted even after 102 h of operation time with 12.24 L volume treated and effluent concentration Cr(VI) of only 7.66 mg/L (38.3% C_o) and column operation was stopped at this point.

Breakthrough curve for total chromium is shown in Fig. 3(b). Throughput volume and mass of chromium removed at exhaustion with respect to total chromium values evaluated using Eqs. (2)–(4) are incorporated in Table 1. From the breakthrough curve of total chromium [Cr(VI) + Cr(III)] [Fig. 3(b)], it can be observed that maximum removal of total chromium was obtained at pH 3 unlike that of pH 2 for Cr(VI). With increase in pH from 2 to pH 3, exhaust time and throughput volume increased from 37 to 45 h and 4.4 to 5.4 L, respectively, with corresponding mass of total chromium removed increased from 16.57 mg to maximum of 26.74 mg. However, with further increase in pH, exhaust time and throughput volume decreased to 23 h and 2.76 L, respectively, at pH 6 with 4.17 mg of total chromium was removed. These findings of maximum Cr(VI) removal at pH 2 but simultaneously less removal for total chromium suggest the reduction of Cr(VI) to Cr(III) at pH 2. Similar trend of maximum total chromium removal at pH 3 by electrostatic attraction of anionic Cr(VI) along with maximum reduction at strong acidic pH 2 was also observed in our previous studies with an amine-based funtionalized polymers viz. aniline formaldehyde condensate (AFC) and polyaniline [19,20]. Biomaterials such as *Ecklonia* biomass were reported to remove Cr(VI) with optimum pH at 3–4 [38,39]. Complete reduction of Cr(VI) to Cr(III) followed by adsorption of the reduced Cr(III) by forming complex with organic materials was reported as the main mechanism of Cr(VI) removal [40,41].

In order to understand the reduction nature of Cr(VI) to Cr(III), concentration of reduced Cr(III) appeared in effluent solution calculated from difference of total chromium and Cr(VI) was plotted against throughput volume along with effluent pH and is shown in Fig. 3(c). At pH 2, maximum concentration of Cr(III) in the effluent was 15 mg/L at a throughput volume of 1.5 L and remained same throughout. However at pH 3, maximum Cr(III) concentration in effluent was only 3.8 mg/L and decreased thereafter with almost no Cr(III) in effluent after throughput volume of 5.5 L. At pH 4, Cr(III) were untraceable after throughput volume of 0.6 L. The total amount of Cr(III) appeared in the effluent till exhaustion was evaluated from the curve of Cr(III) versus throughput volume using Eq. (2) as area below Fig. 3(c) and incorporated in Table 1 (as *M*). Total amount of Cr(III) in effluent that appeared till the exhaustion with respect to total chromium (effluent total chromium 19 mg/L) decreased with increase in pH. At pH 2, mass of Cr(III) in the effluent solution was 62.65 mg and decreased to 6.29 mg at pH 3 followed by insignificant Cr(III) in the effluent at pH 4 and above.

In acidic medium, predominating species of Cr(VI) in the studied pH range (2–6) was the acid chromate ($HCrO_4^-$) form [26]. At this pH, amine group (NH_2) of PANI-jute gets protonated and exists as ammonium ($-NH_3^+$) form. Electrostatic attraction between the protonated ammonium and the negative chromate ions is the plausible mechanism for the removal of Cr(VI) from solution. Therefore, with the decrease in solution pH, protonation of amine sites (NH_2) of PANI-jute increased favoring more electrostatic attraction of negative $HCrO_4^-$ ion yielding high removal of Cr(VI). At influent pH of 2 though PANI-jute was highly protonated, strong acidic environment favored reduction of Cr(VI) to Cr(III) [Eq. (18)]. This positively charged Cr(III) at pH 2 were probably repulsed by protonated PANI-jute and remained in solution (mass of Cr(III) appeared in solution as *M* column in Table 1). To confirm this hypothesis, experiment was carried out using columns with initial Cr(III) of 20 mg/L of influent pH 2 and 3. No removal of Cr(III) were observed confirming the repulsion of reduced Cr(III) by protonated PANI-jute at pH 2 and 3. At influent pH of 3, reduction of Cr(VI) to Cr(III) was much less as compared to influent pH 2 (Table 1) and at pH of 3, anionic adsorption of $HCrO_4^-$ ion with PANI-jute was the predominating mechanism. However, these experimental results are inadequate to justify that form of chromium on PANI-jute surface is in the form of acid chromate [Cr(VI)] as there is still a possibility of reduction of adsorbed Cr(VI) to Cr(III) on the surface of PANI-jute itself. Therefore, further investigation to check the presence of any Cr(III) on PANI-jute surface was carried out by employing ESR technique on both surface of PANI-jute and effluent solution after adsorption experiment at pH 2. The resonance signal of the effluent solution appears at a magnetic field position corresponding to g value of 1.975 [Fig. 3(d)], confirming the presence of Cr(III) whose standard signal *g* value is 1.98 [42]. However, chromium bounded PANI-jute after adsorption experiment showed no peak of Cr(III). Hence, it can be concluded hereby that predominant chromium species on the surface of PANI-jute was Cr(VI) with insignificant or negligible amount of Cr(III).

Interestingly, it was also observed that removal of total chromium was associated with increase of effluent pH from pH 2 to pH 5.57 and pH 3 to 5.54 with insignificant increase when influent pH was 4 and above [Fig. 3(b)]. This result shows that lower

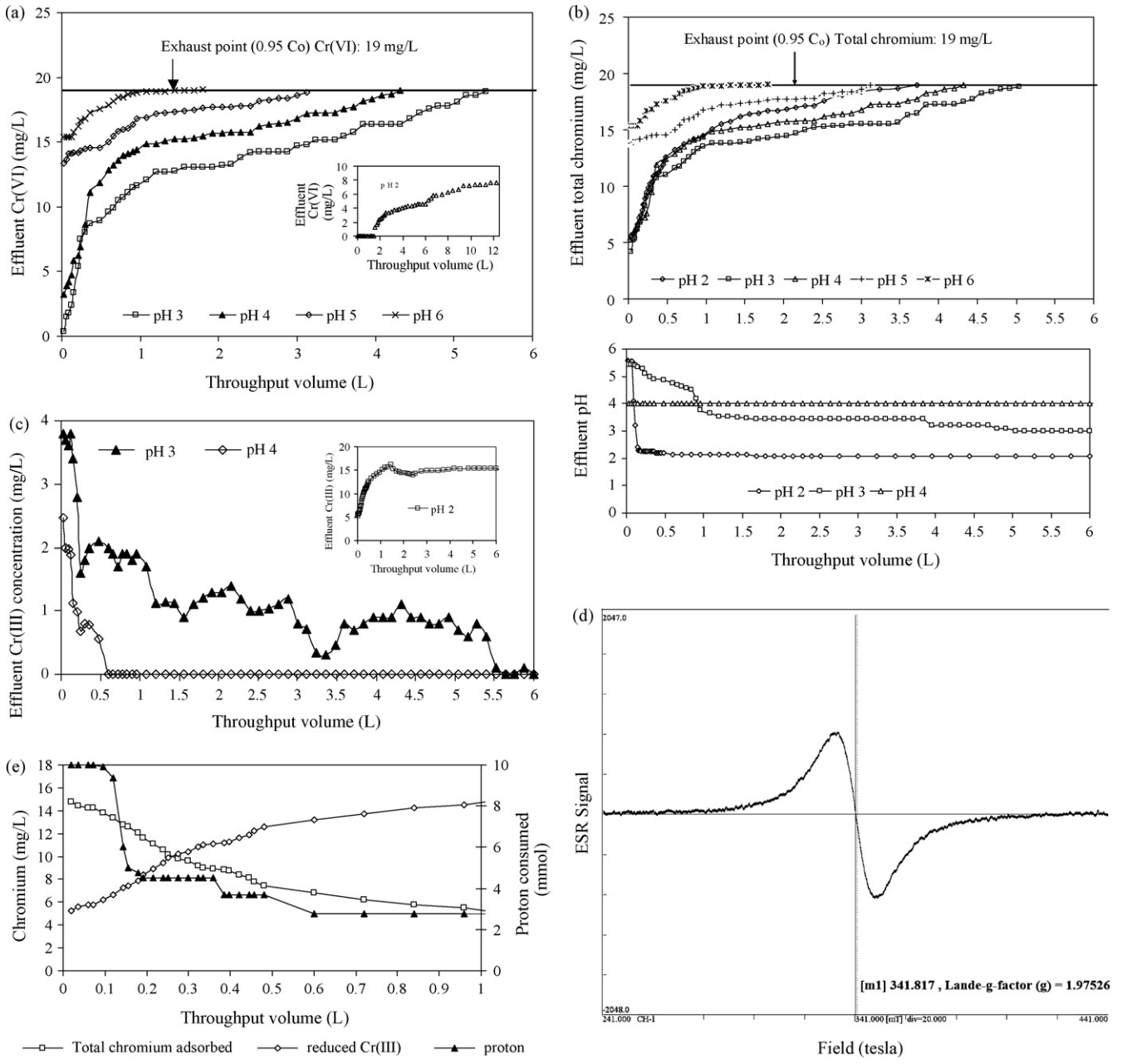

Fig. 3. (a) Effluent Cr(VI) removal by PANI-jute at varying influent pH. (b) Effluent total chromium breakthrough profile and effluent pH at different influent pH. (c) Profile of reduced Cr(III) and pH in the treated effluent (Experiment set 1). (d) ESR spectra of effluent containing Cr(III). (e) Profiles of proton consumption and effluent pH against total chromium adsorbed and Cr(VI) reduced at reaction pH 3.

Table 1
Exhaust time, throughput volume and total uptake of total chromium and Cr(VI) at different pH

Influent pH	Cr(VI)			Total chromium			Cr(III)
	t_E (h)	V_E (L)	M_r (mg)	t_E (h)	V_E (L)	M_r (mg)	M (mg)[a]
2	102[b]	12.24[b]	35.26[b]	37	4.44	16.57	62.65[b]
3	46	5.52	33.20	45	5.40	26.74	6.29
4	39	4.68	21.26	39	4.68	20.66	0.53
5	28	3.36	9.84	28	3.36	9.81	0
6	23	2.76	4.17	23	2.76	4.17	0

[a] Mass of Cr(III) in the effluent was calculated theoretically using Fig. 3(c).
[b] Effluent Cr(VI) concentration was 7.66 mg/L at 102 h and column bed was not exhausted, though column bed was exhausted with respect to total chromium.

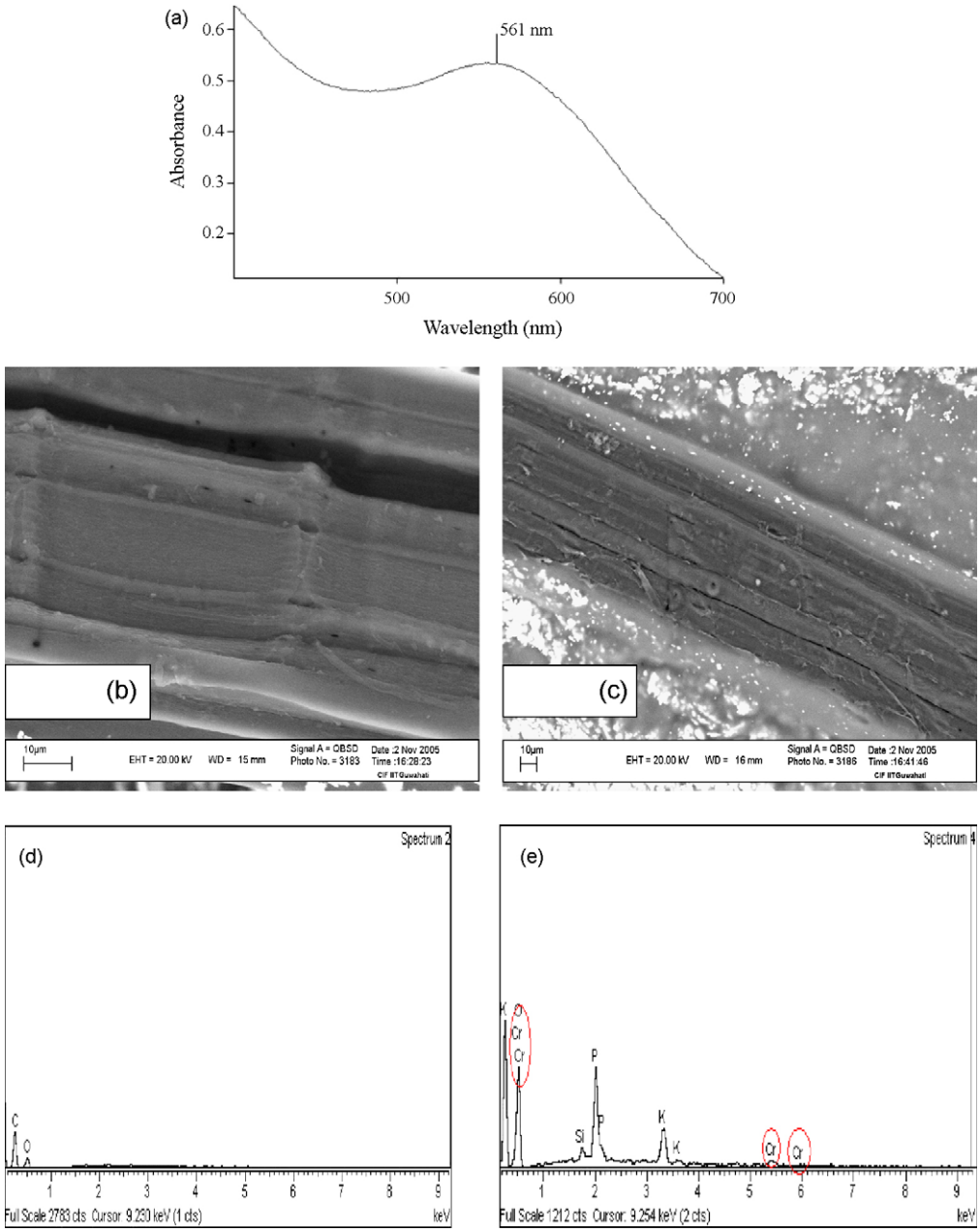

Fig. 4. (a) UV spectra of PANI. (b) and (c) SEM image of PANI-jute before and after chromium adsorption. (d) and (e) EDX of PANI-jute before and after chromium adsorption.

influent pH, higher was proton consumption during chromium removal by PANI-jute. Similar observation was also reported in literatures, where an increase in pH from 2 to 5 was observed during Cr(VI) adsorption by waste acorn in the fixed-bed study [22]. From Table 1 and Fig. 3(b), it was observed that at influent pH of 3 maximum total chromium removal by PANI-jute was achieved. An effort was made to correlate proton consumption (mmol), removal of total chromium (mg/L), appearance of Cr(III) in effluent (mg/L) and throughput volume (L) when column was operated at influent pH of 3 and results are shown in Fig. 3(e). Till throughput volume of 0.12 L, 13–15 mg/L of total chromium has been adsorbed on PANI-jute from influent Cr(VI) 20 mg/L with remaining 5–7 mg/L Cr(III) appeared in

Table 2
Effect of column bed depth on total chromium removal by PANI-jute

Bed depth (cm)	PANI-jute amount (g)	t_B (h)	t_E (h)	V_B (L)[a]	V_E (L)	Amount of total chromium removed [M_r] (mg)	Total chromium uptake [q_e] (mg/g)	EBRT (min)	AER (g/L)[a]
40	9.40	8	82	0.96	9.84	38.87	4.14	15.7	9.79
50	11.75	11	105	1.32	12.6	50.71	4.32	19.65	8.90
60	14.10	20	120	2.40	14.4	65.72	4.66	23.55	5.88

[a] Calculated at 1% breakthrough values.

solution. This observation suggest the adsorption of total chromium predominated over Cr(VI) reduction at initial phase. During this period (up to throughput volume of 0.12 L), 9.9 mmol of protons were consumed. Thereafter, with increase in throughput volume (from 0.12 to 1 L) adsorption of total chromium decreased gradually (from 12 to 5 mg/L of total chromium adsorbed). On the other hand, reduction of Cr(VI) gradually increased with 15 mg/L Cr(III) generated in the effluent at throughput of 1 L and consumed 2.75 mmol protons. Probably with time elapsed and total chromium being adsorbed, active sites of PANI-jute (NH_2) got exhausted and the available protons in the solution were probably utilized for reduction of Cr(VI) to Cr(III). However, these findings of more proton consumption at initial period when adsorption predominated over reduction process and vice versa may be due to requirement of more protons for surface protonation of active sites of PANI-jute than that of protons requirement for reduction process. On study of Cr(VI) adsorption by waste acorn of *Quercus ithaburensis* on a fixed-bed [22] column, the authors estimated chromium by diphenyl carbazide method at 540 nm wavelength by UV spectrophotometer. This technique estimates only Cr(VI) and reduced Cr(III) if any in the solution cannot be evaluated. Similar case was also observed on biosorption of Cr(VI) studies by Motiwal®B30H resin immobilized activated sludge in a packed bed [43]. Since Cr(VI) reduced completely to Cr(III) when contacted with biomaterials [39–41] and adsorbed onto the biomaterials, estimation of total chromium [Cr(VI) + Cr(III)] is also required to evaluate the reduced Cr(III). Analysis of data based on only Cr(VI) estimation will resulted a biased conclusion.

4.2. Characteristics of polyaniline (PANI)

The morphology and chain length of polymer PANI was characterized. PANI synthesized on jute fibers was dissolved in *N*,*N*′-dimethylformamide (DMF) solvent. A UV spectrum of the solvent is taken and is shown in Fig. 4(a). With λ_{max} of 561 nm, the most predominant form of PANI is the short-chain polyaniline (oligoaniline), which have a λ_{max} of 572 nm in DMF solvent [44]. PANI with higher chain length absorbs at 635 nm [45]. The SEM images of PANI-jute before and after chromium adsorption are shown in Fig. 4(b) and (c), respectively. The surface of PANI-jute before adsorption was smooth and even. The energy dispersive X-ray (EDX) analysis for both the PANI-jute samples was also conducted along with SEM to confirm the presence of chromium ion on the surface of PANI-jute [Fig. 4(d) and (e)]. Chromium peaks are visible on the surface of PANI-jute after adsorption experiment, which was absent on the adsorbent surface before interaction with chromium ion.

4.3. Effect of column bed depth

To study the effect of bed depth, experiment were conducted with three columns filled with 9.4, 11.75 and 14.1 g of PANI-jute to yield respective bed depth of 40, 50 and 60 cm and results are shown in Fig. 5. Influent Cr(VI) of 10 mg/L with pH 3 was fed at constant flow rate of 2 mL/min. Details of breakthrough time, exhaustion time, breakthrough volume, exhaustion volume along with amount of total chromium removed and uptake is presented in Table 2. The throughput volumes of total chromium obtained for 40, 50 and 60 cm bed depth at breakthrough point were 0.96, 1.32 and 2.40 L, respectively, and their corresponding exhaust volumes were 9.84, 12.6 and 14.4 L, respectively. At lower bed depth, predominant mass transfer phenomenon was the axial dispersion and reduced the diffusion of chromate ions effectively [46]. Also with increase in bed depth mass transfer zone got broadened as well as more binding sites for adsorption of chromate ions were available. Thus, total

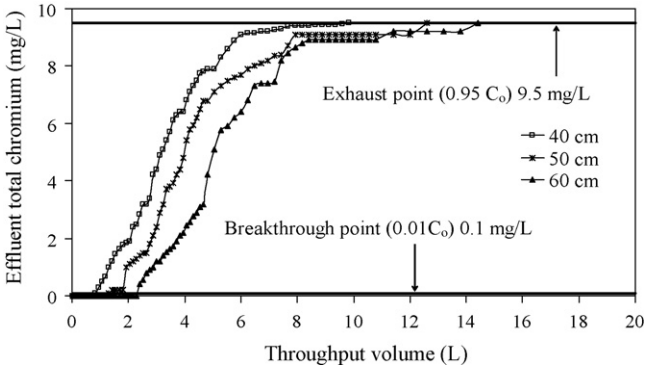

Fig. 5. Breakthrough curves on total chromium removal at various column bed depth.

chromium mass removed (M_r) were evaluated using Eqs. (2)–(4) for column depth of 40, 50 and 60 cm were observed as 38.87, 50.71 and 65.72 mg, respectively.

Table 2 shows that EBRT were 15.7, 19.6 and 23.5 min (at column heights of 40, 50 and 60 cm, respectively). Adsorbent exhaustion rate (AER) was calculated using Eq. (19) for 1% breakthrough.

$$\text{AER (g/L)} = \frac{\text{mass of adsorbent in column (g)}}{\text{throughput volume at breakthrough (L)}} \quad (19)$$

Table 2 shows that when EBRT increased from 15.7 to 19.65 min (25% increase) AER decreased from 9.79 to 8.90 g/L (only 9% decrease). However, when EBRT was further increased to 23.5 min (19.8% increase), AER decreased to 5.88 g/L (33% decrease). Higher EBRT suggests longer residence time, i.e. larger column at the same flow rate, thus indicating more capital cost. Less adsorbent exhaustion rate indicates lower operational cost. From the present experimental observations, optimum column bed height is observed as 60 cm, where with small increase in capital cost caused maximum beneficial effect on lowering operational cost.

Table 2 shows that total chromium uptake by PANI-jute (q_e) calculated using Eq. (5) for bed depth of 40, 50 and 60 cm were 4.14, 4.32 and 4.66 mg/g, respectively. With the increased in bed depth, contact time between the adsorbate and adsorbent increased resulting increase in q_e value. However, uptake (q_e) value obtained from our previous study on batch process showed 62.9 mg/g [20], much higher than uptake value observed in the present work. During biosorption study of Cr(VI) by Mowital®B30H resin immobilized activated sludge at 100 mg/L inlet Cr(VI) concentration, batch system yielded an uptake of 61.0 mg/g as compared to 16.4 mg/g in continuous packed bed studies at flow rate of 0.8 mL/min [43]. Removal of Pb(II) ions by immobilized *Pinus sylvestris* sawdust was reported to achieved an uptake of 7.14 mg/g in batch process as compared to 1.7, 1.6 and 2.2 mg/g at inlet concentrations of 3, 5 and 10 mg/L, respectively, in continuous fixed-bed column [46]. These findings along with the reported literatures suggest that less contact time (residence time) between adsorbate and adsorbent for column mode operation is one of the main reasons for such decrease in uptake value. In actual application of column mode operation such as for treating industrial wastewater, the full bed capacity of column bed cannot be utilized since fixed-bed needs to be changed once the discharge limit or breakthrough is reached. Hence, utilization of full bed is not the main concern in column mode fixed-bed continuous operation. However, to understand the mechanism and nature of metal adsorbent interaction and to analyze the application of mathematical models, running the column operation in lab-scale studies till the exhaust is necessary.

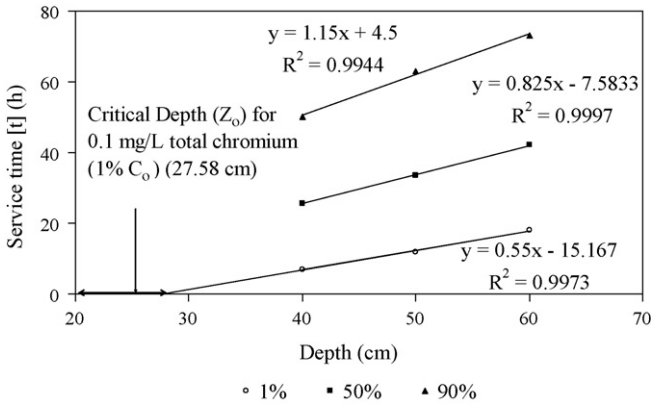

Fig. 6. BDST plot for total chromium adsorption at various breakthrough (Fig. 5 data was used).

4.4. Bed depth service tome (BDST) model

4.4.1. Effect of bed depth

Service time (t_S) and bed depth results are plotted in Fig. 6 according to Eq. (7) for 1%, 50% and 90% breakthrough (calculated from Fig. 5) at column bed depth of 40, 50 and 60 cm. At other breakthrough values also slope, intercepts and correlation coefficients were calculated in a similar way plotting service time and bed depth and results are shown in Table 3.

From Table 3, it can be seen that correlation coefficient values are all above 0.99 suggesting the data fixing on BDST model. There was also a consistent rise in slopes from 0.55 to 1.15 from breakthrough of 1–90% and subsequent increase in corresponding dynamic adsorption capacity N_o from 840.29 to 1756.97 mg/L. At lower breakthrough value, there are some active sites of the polymer still unoccupied by metal ions and thus the adsorbent remained unsaturated. The dynamic adsorption capacity in such low breakthrough condition was therefore bound to be lower than the full bed capacity of the adsorbent. Sharma and Forster [28] reported an increased in slope by 4.72-fold from a breakthrough of 30–70% on removal of Cr(VI) by activated carbon. Similar fact was also observed during removal of lead by granular activated carbon with the slope increase from 12.5 to 35 at breakthrough values of 20–60% [24]. However, Bohart and Adams equation BDST theory assumes a rectangular isotherm having constant dynamic adsorption capacity. Kumar and Bandyopadhyay [47] observed same slopes and constant adsorption capacity N_o for both 10% and 90% breakthrough on removal of Cd(II) by treated rice husk. Constant slope of 0.355 was also reported on removal of phenols by surfactant-modified alumina, thus validating the assumption of constant dynamic adsorption capacity N_o by BDST model [25].

Table 3
Coefficients of BDST equation at different breakthrough

Breakthrough (%)	Slopes	Intercepts	N_o (mg/L)	K (L/mg h)	Coefficient correlation (R^2)
1[a]	0.55	−15.16	840.29	0.03	0.99
10	0.70	−18.33	1069.46	0.01	0.99
20	0.72	−12.25	1107.65	0.01	0.98
30	0.82	−13.41	1260.43	0.01	0.99
40	0.82	−9.91	1260.43	0.004	0.98
50[a]	0.82	−7.58	1260.43	0	0.95
60	0.95	−9.50	1451.41	−0.004	0.97
70	0.95	−4.50	1451.41	−0.02	0.98
80	0.96	3.79	1466.68	0.04	0.99
90[a]	1.15	4.50	1756.97	0.05	0.99

[a] BDST plots for these breakthroughs were also plotted and is shown in Fig. 6.

Another way to examine the application of BDST model is to check the 50% breakthrough curve. At 50% breakthrough, $C_o/C_b = 2$, thus reducing the logarithmic term of BDST equation to zero. Thus, 50% breakthrough curve bounds to pass the origin. Contrastingly, intercept of −7.58 (Table 3) was obtained at 50% breakthrough concluding the non-conformity of BDST models with adsorption of total chromium by PANI-jute. Similar case of non-conformity of Cr(VI) on BDST with respect to 50% breakthrough on removal of Cr(VI) by leaf mould and activated carbon was also reported [28]. All these experimental and literature findings suggest that BDST model cannot be validated only by analyzing the correlation coefficient (R^2). Also the findings suggest that it is not necessary for BDST model to be validated for all breakthrough percentage. Therefore, BDST coefficients of lower breakthrough below 50% can still be utilized for evaluating other parameters such as critical bed depth. Also lower breakthrough below 50% can be fixed on BDST model to design column with different scale process for other flow rates and initial adsorbate concentration without further experimental run [23].

Using Eq. (8), calculated critical bed depth for breakthrough of 1% (0.1 mg/L total chromium) was 27.58 cm. Graphical solution of critical bed depth can also be obtained by extending the best fit linearized line of BDST Eq. (7) to intersect the bed depth axis at $t = 0$ resulting same critical value of 27.58 cm as shown in Fig. 6.

4.4.2. Design of columns for different flow rates

To investigate the validity of BDST model for prediction of different flow rates, two new columns of different flow rates of 1.5 and 2.5 mL/min were operated with same bed depth of 40 cm. Theoretical breakthrough time was obtained by applying data of previous column study at flow rate 2 mL/min using Eq. (9). The comparison between theoretical or predicted and experimental values is shown in Table 4. The predicted value were much in well agreement with experimental value with R.S.D. values of 0.84% and 1.89% for breakthrough of 1% and 10%, respectively, for initial flow rate of 1.5 mL/min. At higher breakthrough, R.S.D. values increased (32% at 90% breakthrough). Similarly predicted breakthrough times for initial flow rate of 2.5 mL/min were also in well agreement with experimental breakthrough for 1% and 10% breakthrough with R.S.D. values of 1.92% and 1.17%, respectively. However, after 10% breakthrough, R.S.D. values also increased to 32–44%. These finding suggest the well conformity of BDST model for total chromium removal by PANI-jute for lower breakthrough till 10%. Inverse relationship has been observed between flow rates and throughput volume for total chromium uptake by PANI-jute. Increase in flow rate from 1.5 to 2.5 mL/min for 1% breakthrough resulted a decreased in contact time from 13 to 2.5 h yielding a decreased in throughput volume from 1170 to 375 mL.

Along with, the amount of total chromium uptake (q_e) was evaluated using Eqs. (2)–(5) and observed that q_e also decreased from 4.45 to 3.26 mg/g with increased in flow rate from 1.5 to 2.5 mL/min. At higher flow rate, contact time between PANI-jute and chromate ions decreased resulting lesser intra-particular diffusion of metal ions on PANI-jute. This led to an early breakthrough and early saturation of column bed yielding less adsorption.

4.4.3. Design of columns for different initial concentrations

Degree of predictability for different scale initial concentration of Cr(VI) by BDST model was checked by conducting running two columns with different influent Cr(VI) of 5 and 15 mg/L at flow rate of 2 mL/min and column bed depth 40 cm. Theoretical breakthrough time were obtained from previous column study conducted at same flow rate 2 mL/min, depth 40 cm and influent Cr(VI) 10 mg/L. Using Eqs. (10) and (11), theoretical slopes and intercepts were calculated and breakthrough times for both 5 and 15 mg/L initial Cr(VI) concentration were evaluated (Table 4).

Table 4
Comparison of experimental and theoretical breakthrough time using BDST model for total chromium adsorption using PANI-jute

Breakthrough (%)	Flow rate 1.5 mL/min			Flow rate 2.5 mL/min			Initial Cr(VI) 5 mg/L			Initial Cr(VI) 15 mg/L		
	t_{exp} (h)[a]	t_{theo} (h)[b]	R.S.D (%)[c]	t_{exp} (h)[a]	t_{theo} (h)[b]	R.S.D. (%)[c]	t_{exp} (h)[a]	t_{theo} (h)[b]	R.S.D. (%)[c]	t_{exp} (h)[a]	t_{theo} (h)[b]	R.S.D. (%)[c]
1	13	14.2	0.84	2.5	2.4	1.92	19	19.4	1.82	3.5	3.4	1.67
10	18.5	19.0	1.89	3	4.1	1.17	26	26.8	1.03	5	5.1	0.98
50	26	36.4	23.60	9.8	18.8	44.56	30	53.7	40.1	20	16.4	14.08
90	105	65.8	32.42	66	41.3	32.55	160	99.2	33.1	47	34	22.68

[a] t_{exp}, Experimental breakthrough time (h).
[b] t_{theo}, Theoretical breakthrough time (h).
[c] R.S.D., Relative standard deviation percentage (standard deviation × 100/average).

Predicted breakthrough time were much in agreements with the experimental breakthrough time with R.S.D. value of 1.82% and 1.03% at breakthrough of 1% and 10%, respectively, for initial Cr(VI) 5 mg/L. Similarly for Cr(VI) 15 mg/L, R.S.D. value of 1.67% and 0.98% for breakthrough of 1% and 10%, respectively, were obtained. However, R.S.D. value of 5–40.1% for both initial Cr(VI) concentration of 5 and 15 mg/L suggest the conformity of BDST model till 10% breakthrough. With the increase in influent Cr(VI) from 5 to 15 mg/L corresponding 1% breakthrough time decreased from 19 to 3.5 h with the subsequent decrease of throughput volume from 2.28 to 0.42 L. At higher influent Cr(VI), fixed-bed got saturated with chromate ions more quickly thereby decreasing the breakthrough and exhaustion time. However, q_e value increased from 4.14 to 5.02 mg/g total chromium with increase in influent concentration from 5 to 15 mg/L. Probably at higher concentration of chromate, loading rate increased even though contact time decreased and the net effect was an appreciable increase in adsorption capacity. These suggest that initial concentration of adsorbate effects the diffusion of adsorbate in adsorbent.

4.5. Thomas model

Data of different column depth were also treated with Thomas model [Eq. (13)] and coefficients and calculated q_e value are presented in Table 5. Predicted and experimental value were well agreed with less R.S.D. value for column studied with flow rate 2 mL/min and initial Cr(VI) 10 and 15 mg/L. However, the results of columns with flow rate of 1.5 and 2.5 mL/min with initial Cr(VI) 10 mg/L and column with flow rate of 2 mL/min and initial Cr(VI) 5 mg/L were not following on Thomas model (R^2 value of less than 0.7). This probably may be stems due to its derivation from second-order reversible reaction kinetics which usually is not limited by chemical reaction kinetics but is often controlled by inter phase mass transfer [32,48].

4.6. Theoretical breakthrough curve

The theoretical breakthrough was generated with the initial concentration of 10 and 20 mg/L following the concepts of Michaels [33] as follows:

(1) The equilibrium line was prepared using Langmuir's adsorption isotherm of our previous batch work of total chromium removal by PANI-jute [20]:

$$q_e = \frac{q_m b C_e}{1 + b C_e} \quad (20)$$

where q_e (mg/g) is the amount of total chromium ions adsorbed per unit weight of PANI-jute, q_m the maximum monolayer coverage which equals to 162.89 mg/g, b the energy (heat) constant of adsorption (L/mg) which equals to 0.02 L/mg, and C_e is the equilibrium concentration of Cr(VI) ion remaining in solution (mg/L).
(2) An operating line was drawn passing through the origin and intersecting the equilibrium curve at C_o of 10 and 20 mg/L yielding respective q_e values of 10.48 and 17.96 mg/g [Fig. 7(a)].
(3) A graph of C versus $(C - C_e)^{-1}$ was plotted where the area under the curve of $(C - C_e)^{-1}$ represented the value of the integration of Eq. (14) and is shown in Fig. 7(b). For initial Cr(VI) of 10 and 20 mg/L, 41.48 and 17.48 sq. units were obtained, respectively.
(4) Using Eq. (16), the theoretical breakthrough curves were generated by plotting $(V_t - V_B)/(V_E - V_B)$ versus (C/C_o). It can be seen in Fig. 7(c) that for both the initial Cr(VI) of 10 and 20 mg/L, the experimental and theoretical breakthrough curves followed the same trend.

4.7. Desorption and recovery

The recovery of metal ions from the metal saturated bed was another important aspect for reusability of adsorbent to reduce the process cost. Before starting the desorption experiment, one adsorption experiment was carried out with three column of 20, 30 and 40 cm depth initially fed with 20 mg/L Cr(VI) at 2.5 mL/min flow rate till exhaust. The exhausted adsorbent was used for desorption study. Desorption study was conducted with desorbent of 1 M NaOH at lower flow rate of 1 mL/min. Lower flow rate was applied so as to access more contact time and concentrate the chromate ions in possible minimum volume. A plot of throughput volume of desorbents versus concentration of total chromium recovered is shown in Fig. 8. From the figure, effluent total chromium concentration was observed to be decreased with time elapsed. After throughput

Table 5
Coefficients of Thomas model for total chromium adsorption by PANI-jute

Bed height (cm)	Initial Cr(VI) (mg/L)	Flow rate (mL/min)	t_B (h)	t_E (h)	Thomas model				
					k_{TH} (mL min^{-1} g^{-1})	R^2	$Q_{o,exp}$ (mg/g)	$Q_{o,theo}$ (mg/g)	R.S.D. (%)
40	10	2	8	82	0.012	0.98	4.14	3.73	7.3
50	10	2	11	105	0.010	0.95	4.32	3.95	6.3
60	10	2	20	120	0.008	0.96	4.66	4.37	4.5
40	10	1.5	14	130	0.023	0.49	4.45	3.56	15.7
40	10	2.5	2.5	78	0.067	0.55	3.26	1.987	34.3
40	5	2	19	190	0.025	0.69	3.7	0.265	122.5
40	15	2	3.5	64	0.006	0.93	5.02	4.67	5.1

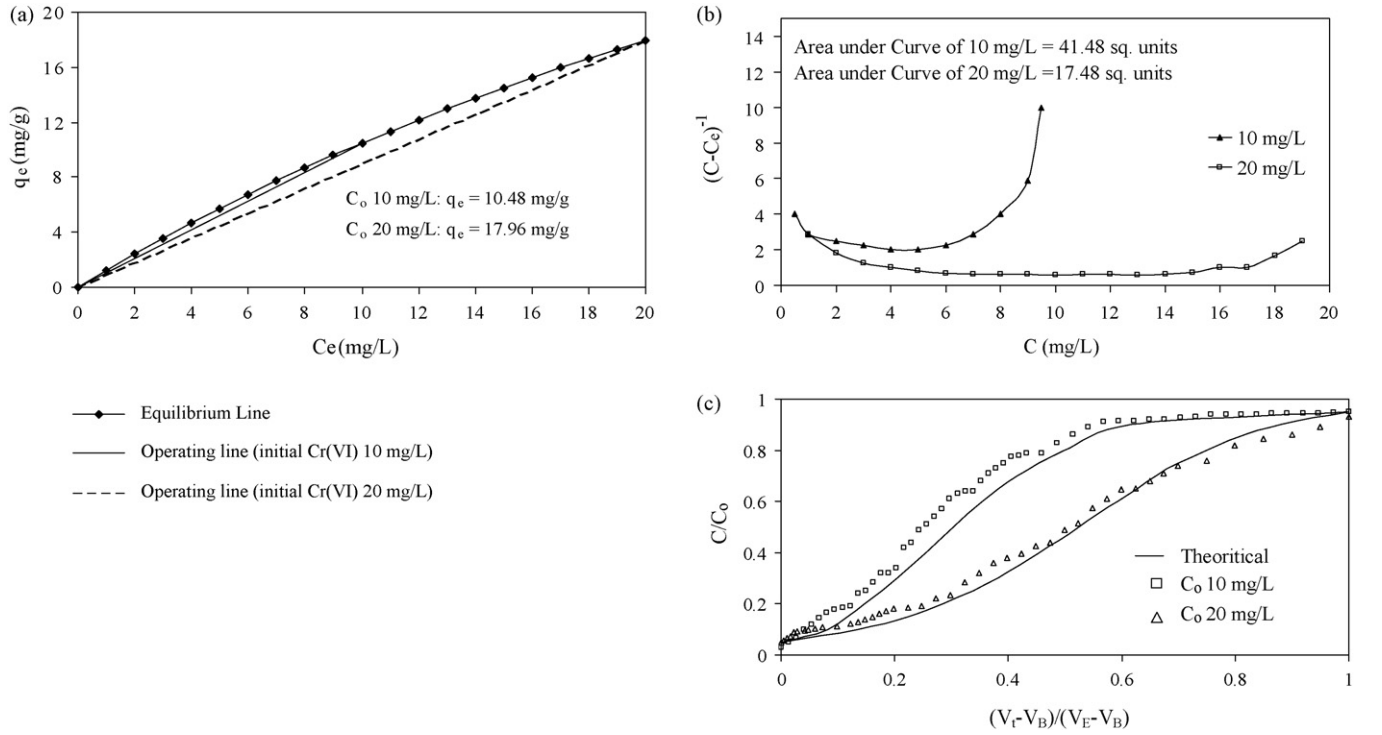

Fig. 7. (a) Equilibrium and operating lines to predict breakthrough curve. (b) Curve area to evaluate for determination of theoretical breakthrough curve of total chromium. (c) Theoretical and experimental breakthrough curve of total chromium.

volume of 0.42 L (7 h of desorption operation), there were no further total chromium traced in the effluent. Thus, all chromate ions were able to concentrate on 0.42 L of desorbent. Amount of desorption was estimated using Eq. (21) as:

$$\text{desorption}\,(\%) = \frac{M_d}{M_r} \times 100 \tag{21}$$

where M_d and M_r are the amount of total chromium desorbed and adsorbed (mg), respectively. 2.48%, 3.08% and 2.99% of total chromium were desorbed at 20, 30 and 40 cm of column bed depth respectively. This value was much lower than value observed in batch study, where almost 83% desorption was observed while using 2 M NaOH in 10 min [20]. Probably increasing NaOH strength further or desorption in batch process may recover back more total chromium. During desorption by alkali, $HCrO_4^-$ ion attached to protonated surface of PANI-jute by electrostatic attraction were probably replaced by OH^- and remained in the solution. Such less desorption also indicates the possibility of strong binding of metal ions on active sites of PANI-jute.

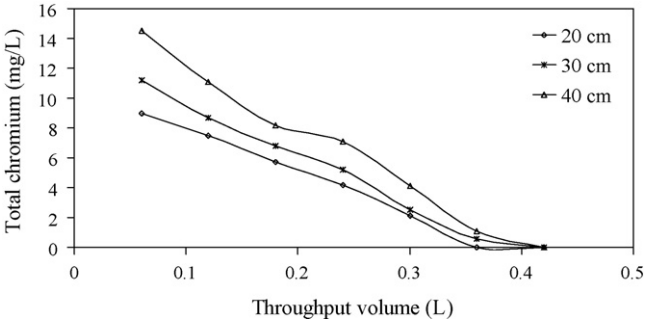

Fig. 8. Desorption profiles at different bed depth.

Solid waste management of toxic metal contaminated is a primary concern which otherwise will pollute the soil and then the groundwater. Recovery of the adsorbed metals by igniting the metal contaminated adsorbent is another viable alternative. To investigate the degree of recovery of chromate ions, exhausted PANI-jute fibers from 40, 50 and 60 cm bed depth weighing 9.4, 11.75 and 14.1 g, respectively, were subjected to ignition in muffle furnace at 550 °C for 1 h. Weight of PANI-jute-chromium of all three different bed depth decreased to only 0.2 g reducing the weight by 97.5–98.5%. There is a chance of leakage of chromate ions into the environment from the adsorbent after adsorption and ignition. The ash (0.2 g) obtained after ignition were therefore dissolved in 1N HNO_3 and the sample was analyzed for chromate ions. Interestingly, it was observed that all the adsorbed chromate ions were recovered back in the solution, however, in non-toxic Cr(III) form. It is possible to remove toxic Cr(VI) from wastewater by PANI-jute by adsorption. This study results will help to design fixed-bed columns for large scale Cr(VI) containing industrial wastewater.

5. Conclusions

In this study, an extensive laboratory investigation was conducted to evaluate fixed-bed column performance for the removal of hexavalent chromium [Cr(VI)] from aqueous solution. A short-chain polymer, polyaniline was synthesized by adding formaldehyde in aniline solution under acidic medium on the surface of jute fiber and this polyaniline-jute (PANI-jute) was used as an adsorbent in the fixed-bed columns. Influent pH, column bed depth, influent Cr(VI) concentrations and influent flow rate were variable parameters for the present study and based on the findings of this study following conclusions can be drawn:

(1) Optimum pH for total chromium [Cr(VI) + Cr(III)] removal was obtained at pH 3 with removal of 26.74 mg total chromium at flow rate of 2 mL/min and initial Cr(VI) 20 mg/L. At pH 2, Cr(VI) were largely reduced to Cr(III) and remained in solution with total chromium removal of only 16.57 mg/g. Electrostatic attraction of acid chromate ion ($HCrO_4^-$) with protonated amine group (NH_3^+) of PANI-jute was the main mechanism of Cr(VI) removal at pH 3. EDX and ESR spectra confirmed presence of chromium on the surface of PANI-jute in the form of Cr(VI).
(2) The data obtained for total chromium were well described by BDST equation till 10% breakthrough. Adsorption rate constant and dynamic bed capacity at 10% breakthrough were observed as 0.01 L/mg h and 1069.46 mg/L, respectively. Critical bed depth of adsorbent that would be able to prevent the chromium concentration from exceeding the permissible limit was obtained as 27.58 cm at flow rate of 2 mL/min and initial Cr(VI) 10 mg/L.
(3) The experimental breakthrough profile was in good agreement with theoretical breakthrough profile obtained from batch data incorporated into Langmuir isotherm model.
(4) All the adsorbed total chromium was recovered back as oxides of chromium by ignition of chromium loaded PANI-jute along with more than 97% reduction in weight of PANI-jute. PANI-jute can be used effectively to remove the chromium and keeps the effluent well below the permissible limit along with minimum solid waste management of toxic metal loaded adsorbent.

Acknowledgement

Dr. Saswati Chakraborty would like to thank Council of Scientific and Industrial Research (CSIR), Govt. of India (No. 22 (0418)/06/EMR-II) for financial support to this work.

Appendix A. Supplementary data

Supplementary data associated with this article can be found, in the online version, at doi:10.1016/j.jhazmat.2008.05.147.

References

[1] WHO, Guidelines for Drinking-Water Quality, World Health Organization, Geneva, 1993.
[2] IS 10500:1991, Drinking Water Specifications, Bureau of Indian Standards, New Delhi, 1991.
[3] L. Khezami, R. Capart, Removal of chromium(VI) form aqueous solution by activated carbons: kinetic and equilibrium studies, J. Hazard. Mater. 123 (2005) 223–231.
[4] X. Zhou, T. Korenaga, T. Takahashi, T. Moriwake, S. Shinoda, A process monitoring/controlling system for the treatment of wastewater containing chromium(VI), Water Res. 27 (1993) 1049–1054.
[5] J.C. Seaman, P.M. Bertsch, L. Schwallie, In situ Cr(VI) reduction within coarse-textured, oxide-coated soil and aquifer systems using Fe(II) solutions, Environ. Sci. Technol. 33 (1999) 938–944.
[6] N. Kongsricharoern, C. Polprasert, Chromium removal by a bipolar electrochemical precipitation process, Water Sci. Technol. 34 (1996) 109–116.
[7] A. Tor, T. Büyükerkek, Y. Cengelolu, M. Ersöz, Simultaneous recovery of Cr(III) and Cr(VI) from the aqueous phase with ion-exchange membranes, Desalination 171 (3) (2005) 233–241.
[8] K. Pagilla, L.W. Canter, Laboratory studies on remediation of chromium-contaminated soils, J. Environ. Eng. 125 (1999) 243–248.
[9] Z. Aksu, T. Kutsal, A comparative study for biosorption characteristics of heavy metal ions with *C. vulgaris*, Environ. Technol. 11 (1990) 979–987.
[10] Z. Aksu, D. O¨zer, H. Ekiz, T. Kutsal, A. Calar, Investigation of biosorption of chromium(VI) on *C. crispate* in two-staged batch reactor, Environ. Technol. 17 (1996) 215–220.
[11] S.F. Montanher, E.A. Oliveira, M.C. Rollemberg, Removal of metal ions from aqueous solutions by sorption onto rice bran, J. Hazard. Mater. B117 (2005) 207–211.
[12] M. Dakiky, M. Khamis, A. Manassra, M. Mer'eb, Selective adsorption of chromium(VI) in industrial wastewater using low-cost abundantly available adsorbents, Adv. Environ. Res. 6 (2002) 533–540.
[13] T. Karthikeyan, S. Rajgopal, L.R. Miranda, Chromium(VI) adsorption from aqueous solution by Hevea Brasilinesis sawdust activated carbon, J. Hazard. Mater. 124 (2005) 192–199.
[14] S. Deng, R. Bai, Removal of trivalent and hexavalent chromium with animated polyacrylonitrile fibers: performance and mechanisms, Water Res. 38 (2004) 2424–2432.
[15] C. Jeon, W.H. Holl, Chemical modification of chitosan and equilibrium study for mercury ion removal, Water Res. 37 (2003) 4770–4780.
[16] B. Mathew, V.N.R. Pillai, Polymer–metal complexes of amino functionalized divinylbenzene-crosslinked polyacrylamides, Polymer 34 (12) (1993) 2650.
[17] P. Viel, S. Palacina, F. Descoursb, C. Bureaub, F.L. Derf, J. Lyskawac, M. Salle, Electropolymerized poly-4-vinylpyridine for removal of copper from wastewater, Appl. Surf. Sci. (212–213) (2003) 792–796.
[18] M. Chanda, G.L. Rempel, Polyethyleneimine gel-coat on silica: high uranium capacity and fast kinetics of gel-coated resin, React. Polym. 25 (1995) 25–36.
[19] P.A. Kumar, M. Ray, S. Chakraborty, Hexavalent chromium removal from wastewater using aniline formaldehyde condensate coated silica gel, J. Hazard. Mater. 143 (2007) 24–32.
[20] P.A. Kumar, M. Ray, S. Chakraborty, Removal and recovery of chromium from wastewater using short chain polyaniline synthesized on jute fiber, Chem. Eng. J. 141 (2008) 130–140.
[21] J.P. Chen, J.-T. Yoon, S. Yiacoumi, Effects of chemical and physical properties of influent on copper sorption onto activated carbon fixed-bed columns, Carbon 41 (2003) 1635–1644.
[22] E. Malkoc, Y. Nuhoglu, Cr(VI) adsorption by waste acorn of *Quercus ithaburensis* in fixed beds: prediction of breakthrough curves, *Y. abali*, Chem. Eng. J. 119 (2006) 61–68.
[23] K. Vijayaraghavan, J. Jegan, K. Palanivelu, M. Velan, Batch and column removal of copper from aqueous solution using a brown marine alga *Turbinaria ornate*, Chem. Eng. J. 106 (2005) 177–184.
[24] J. Goel, K. Kadirvelu, C. Rajagopal, V.K. Garg, Removal of lead(II) by adsorption using treated granular activated carbon: batch and column studies, J. Hazard. Mater. B125 (2005) 211–220.
[25] A. Adak, A. Pal, Removal of phenol from aquatic environment by SDS-modified alumina: batch and fixed bed studies, Sep. Purif. Technol. 50 (2) (2006) 256–262.
[26] L.D. Benefield, J.F. Judkins, B.L. Weand, Process Chemistry for Wastewater Treatment, Prentice-Hall, Englewood Cliffs, NJ, 1982, pp. 433–439.
[27] A.P. Sincero, G.A. Sincero, Physical–Chemical Treatment of Water and Wastewater, CRC press, Florida, USA, 2003, pp. 401–402.
[28] D.C. Sharma, C.E. Forster, A comparison of the sorbtive characteristics of leaf mould and activated carbon columns for the removal of hexavalent chromium, Process. Biochem. 31 (1996) 213–218.
[29] V. Sarin, T.S. Singh, K.K. Pant, Thermodynamic and breakthrough column studies for the selective sorption of chromium from industrial effluent on activated eucalyptus bark, Bioresour. Technol. 97 (2006) 1986–1993.
[30] G.S. Bohart, E.Q. Adams, Some aspects of behavior of charcoal with respect to chlorine, J. Am. Chem. Soc. 42 (1920) 523–529.
[31] R.A. Hutchin, New simplified design of activated carbon systems, Am. J. Chem. Eng. 80 (1973) 133–138.
[32] H.C. Thomas, Heterogeneous ion exchange in a flowing system, Am. Chem. Soc. 66 (1994) 1664–1666.
[33] A.S. Michaels, Simplified method of interpreting kinetic data in fluid bed ion exchange, Ind. Eng. Chem. 44 (1952) 1922.
[34] W.J. Weber Jr., Physico-chemical Process for Water Quality Control, Wiley Inc., 1972, pp. 261–305.
[35] X. Yang, T. Zhao, Y. Yu, Y. Wei, Synthesis of conductive polyaniline/epoxy resin composites: doping of the interpenetrating network, Synth. Mater. 142 (2004) 57–61.
[36] D.C.K. Ko, J.F. Porter, G. McKay, Optimised correlations for the fixed-bed adsorption of metal ions on bone char, Chem. Eng. Sci. 55 (2000) 5819–5829.
[37] APHA, WEF and AWWA, Standard Methods for the Examination of Water and Wastewater, 20th ed., APHA, Washington, DC, USA, 1998.
[38] D. Park, Y.S. Yun, J.M. Park, Reduction of hexavalent chromium with the brown seaweed *Ecklonia* biomass, Environ. Sci. Technol. 38 (2004) 4860–4864.
[39] D. Park, Y.S. Yun, K.H. Yim, J.M. Park, Effect of Ni(II) on the reduction of Cr(VI) by *Ecklonia* biomass, Bioresour. Technol. 97 (2006) 1592–1598.
[40] D. Park, Y.S. Yun, K.H. Yim, J.M. Park, How to study Cr(VI) biosorption: use of fermentation waste for detoxifying Cr(VI) in aqueous solution, Chem. Eng. J. 136 (2008) 173–179.
[41] D. Park, Y.S. Yun, J.M. Park, Mechanisms of the removal of hexavalent chromium biomaterials or biomaterial-based activated carbon, J. Hazard. Mater. B137 (2006) 1254–1257.
[42] W.G. Bryson, Application of electron spin resonance in the analytical chemistry of transition metal ions, Part 3. Determination of chromium(III) in aqueous solution, Anal. Chim. Acta 116 (1980) 353–357.
[43] Z. Aksu, F. G¨onen, Z. Demircan, Biosorption of chromium(VI) ions by Mowital®B30H resin immobilized activated sludge in a packed bed: comparison with granular activated carbon, Process. Biochem. 38 (2002) 175–186.
[44] Y. Wei, C. Yang, T. Ding, A one-step method to synthesize *N,N′*-bis(4′-aminophenyl)-1,4-quinonenediimine and its derivatives, Tetrahedron Lett. 37 (1996) 731–734.

[45] T.A. Huber, A Literature Survey of Polyaniline, Part 1 Polyaniline as a Radar Absorbing Material, Defence R&D Canada—Atlantic, Technical Memorandum, DRDC Atlantic TM, January 2003, pp. 2003–2014.
[46] V.C. Taty-Costodes, H. Fraduet, C. Porte, Y.S. Ho, Removal of lead(II) ions from synthetic and real effluents using immobilized *Pinus sylvestris* sawdust: adsorption on a fixed-bed column, J. Hazard. Mater. B123 (2005) 135–144.
[47] U. Kumar, M. Bandyopadhyay, Fixed bed column study for Cd(II) removal from wastewater using treated rice husk, J. Hazard. Mater. 129 (1–3) (2006) 253–259.
[48] J.R. Rao, T. Viraraghavan, Biosorption of phenol from a aqueous solution by *Aspergillus niger* biomass, Bioresour. Technol. 85 (2002) 165–171.